21st IAEA Fusion Energy Conference: Summary on Sessions EX/D, EX/S and EX/W

Hartmut Zohm

MPI für Plasmaphysik, D-85748 Garching, Germany, EURATOM Association

e-mail contact of main author: zohm@ipp.mpg.de

1. Introduction

This paper summarises the main results presented in the 21st IAEA Fusion Energy Conference in Chengdu, China, in October 2006 concerning the topics EX/D (Experimental Divertor Physics and Plasma Wall Interaction), EX/S (Experiments on Stability) and EX/W (Experiments on Waves and Fast Particles). It summarises a total of 92 papers, givenas orals and posters in Chengdu. In preparing this summary, the author has tried to identify the most important subtopics in these areas and highlighted the new results. This means that not all papers presented at the conference under these topics are dealt with explicitly.

2. Session EX/D: Experimental Divertor Physics and Plasma Wall Interaction

The contributions to this session mainly dealt with the fields of 'bursty' SOL transport, retention of hydrogenic fuel, alternative (to C) wall materials and divertor physics. Other topics presented, but not dealt with in this summary paper, comprise the migration of wall material and in particular the characterisation and behaviour of dust in fusion experiments.

2.1 Bursty SOL transport

In this area, many new experimental results were presented from Alcator C-Mod [1], ASDEX Upgrade [2], DIII-D [3], JET [4], JT-60U [5], LHD [6] and MAST [7] and NSTX [3]. The phenomenon of 'bursty' transport in the SOL refers to the observation that the flux of energy and particles across the separatrix into the SOL is in general not continuous, but occurs in intermittent, clearly distinct events on top of a more or less pronounced background.

Experimental observations of bursty transport in the SOL are reported during both L- and H-mode as well as during ELMs. They are observed in tokamaks as well as in stellarators, indicating a fundamental nature of the phenomenon to toroidal magnetically confined plasmas. In L- and H-mode they are interpreted as intermittent structures evolving from turbulent transport that drives heat and articles across the separatrix, whereas in ELMs, they are most likely driven by the nonlinear ELM stage, which follows the linear onset characterised by a more or less well-defined single intermediate (n=5-10) MHD instability that is also sometimes observed as precursor oscillations. Fig. 1 shows an example from the MAST spherical torus, where bursty structures recorded by a high-speed camera are shown during L-mode (left) and an ELM (right). From these figures, it can clearly be seen that the structures are localised along magnetic field lines with a sharp localisation in poloidal angle, i.e. they have high k_{perp} and small k_{par}. This spatial structure has also led to the usage of the term 'filament' for these structures. Analysis of the temporal evolution of the radial and toroidal position of individual filament show that they are decelerated toroidally and

accelerated radially as they travel through the SOL. This is consistent with an interpretation of interchange instabilities on open field lines in this phase of the event.

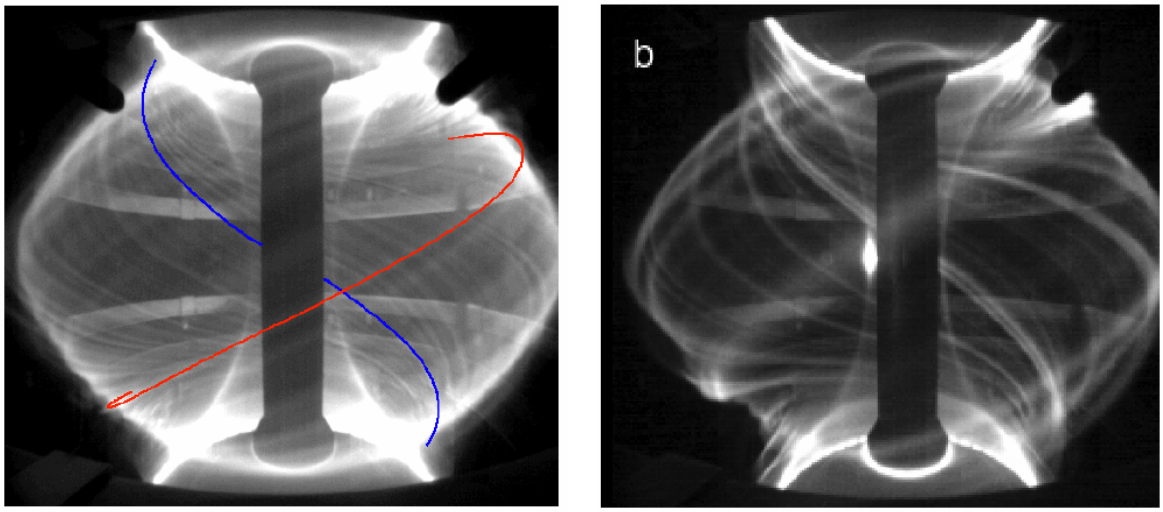

FIG 1. High speed camera snapshots of bursty SOL transport during L-mode (left) and H-mode (right) in the MAST spherical torus.

These findings have several implications for transport in the SOL. In particular, they offer a possible explanation for the long-standing observation of two decay lengths in the SOL, one with a large value leading to the existence of plasma in the far SOL wings. This is now interpreted as a result of the fast conduction along field lines that leads to the short decay length in competition with the radial transport due to bursts, which is responsible for the long decay length. In particular, also the sharing of power loads on target plates and main chamber PFCs in ELMs is interpreted as a result of the competition between these two processes, with about 20% of the power load reaching the main chamber while 80% reach the target plates. This picture may in fact give first hints towards a nonlinear theory of the ELM evolution.

Finally, filaments, that occur preferentially on the low field side, also explain the observed asymmetry in outflux, which occurs preferentially on the mid-plane outside. This was documented in detail on Tore Supra [8], where particle fluxes measured by a Mach probe with different limiting points were only consistent with a localised outflux in the midplane, but not with a poloidally uniform model.

2.2 Retention of hydrogenic fuel

Several experimental results clearly confirm earlier findings that a significant fraction of hydrogenic fuel is stored in the first wall during operation. Figure 2 presents evidence from Tore Supra and ASDEX Upgrade showing that in global gas balance, between 10 % and 40 % of the injected hydrogenic fuel can be trapped in the wall [9]. For the Tore Supra case, it is shown that outgassing in between shots cannot account for the missing inventory. These findings are supported by post-mortem analysis of C-tiles form JET [10], which finds retention of hydrogenic fuel of the order of 3-5 %, which is of course only representative of a fraction of the total retention. Two main processes are discussed for this 'quasi-permanent' storage of hydrogenic fuel, namely bulk diffusion in the wall material that leads to deep trapping (especially important for CFC as is the case in Tore Supra) and hydrogenic co-deposition by carbo-hydrates that reach remote areas of the vessel and lead to the formation of

films there, ultimately even producing flakes that have been found at the bottom of the vacuum vessel in several devices.

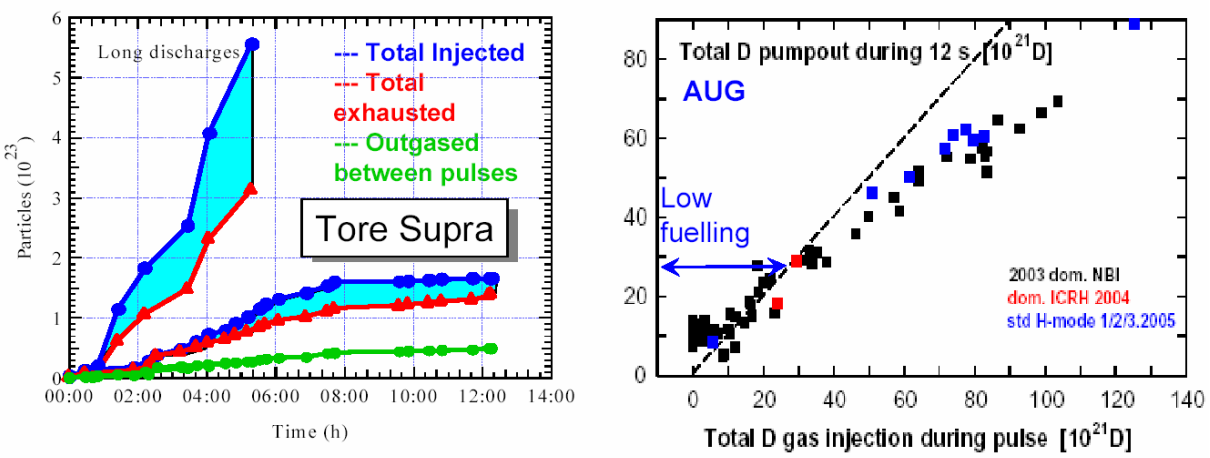

FIG. 2: Gas balance in Tore Supra (left) and ASDEX Upgrade (right). Both experiments find a significant retention of hydrogenic fuel in the wall.

Several strategies are being discussed how to minimise the retention, amongst them avoidance of formation of films of hydrocarbons by heating the surfaces prone to this effect [11], cleaning techniques such as laser irradiation or even provoked disruptions [12] or the use of non-C wall materials. The latter will be discussed in the next section.

2.3 Alternative (non-C) wall materials

Several papers dealt with the use of non-C wall materials, triggered by the above mentioned problem of co-deposition of hydrogenic fuel in devices with a C-wall, but also by the need to use wall materials with low erosion rates; the present status of DEMO studies is that a high-Z wall is absolutely mandatory there and thus also in a reactor [13].

High Z walls are studied in Alcator C-Mod (Mo) [14] and ASDEX Upgrade (W) [15]. Both machines reported increased influx of high Z-impurities from the protection limiters of the ICRH antennae, caused by the acceleration of high-Z ions due to the sheath potential in front of the antenna. For C-Mod (where ICRH is the main heating mehod), this leads to a rapid decrease in plasma performance after boronisation as shown in Fig. 3. The situation is less severe in ASDEX Upgrade where NBI can be used as main heating method, but a clearer assessment of the situation will be done there with the full W-covered first wall in 2007.

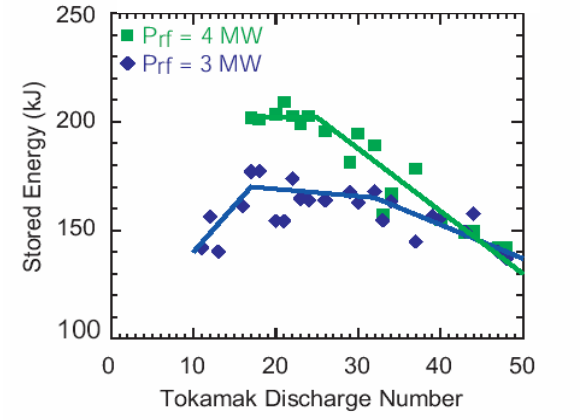

FIG. 3: Decrease of plasma performance, measured by the stored energy in identical discharges performed after boronisation in Alcator C-Mod.

First results of the use of liquid-Li limiters were reported from FTU [16] and T-11M [17], where FTU did not find deleterious impact on plasma performance. It could be shown that the limiter temperature saturated at lower values than expected, probably due to a 'self-shielding' effect of Li. On the contrary, due to the gettering effect due to Li, pumping capability was effectively improved and discharges close to the Greenwald limit could be performed with good plasma performance. These encouraging results will of course have to be confirmed in future experiments on larger scale.

2.4 Divertor physics

Several results in the area of divertor physics were presented. Perhaps the most striking result was the largely improved performance of LHD discharges after introduction of an island divertor [18]. This allowed good pumping and thus better edge density control, giving access to a regime in which the central density could greatly be improved in conjunction with pellet fuelling. The regime was dubbed IDB (Internal Diffusion Barrier) regime and led to new record values of stored energy in fusion triple product in LHD, despite the substantial reduction of plasma volume due to the island divertor.

3. Session W: Waves and fast particles

In the area of waves and fast particles, increasing attention is given to the interaction between waves and fast particles, a subject that will be a focus point of ITER research. Here, waves do not only refer to high frequency electromagnetic waves, but also to low frequency MHD activity which can interact with fast particles. In addition, a number of papers was presented on wave heating and current drive, both in tokamaks, but also for alternative concepts.

3.1 Interaction of MHD instabilities with fast particles

The interaction of MHD instabilities with fast particles is twofold, since on the one hand, MHD instabilities can redistribute or even eject fast particles, but on the other hand, gradients of the fast particle distribution, both in real space and in velocity space, can excite MHD instabilities. Usually, MHD instabilities are driven by fast ions, because the typical frequencies of ion orbits, such as e.g. banana precession or banana transit time, lie in the range of typical MHD mode frequencies, leading to resonant condition for excitation or redistribution. However, recently, also electron related instabilities have been observed such as the electron fishbones in HL-2A or FTU [19], which are related to particular orbits, where barely trapped electrons can change the direction of their precession due to their long residence time on the high field side. Fig. 4 shows an example of electron fishbones during LHCD in FTU.

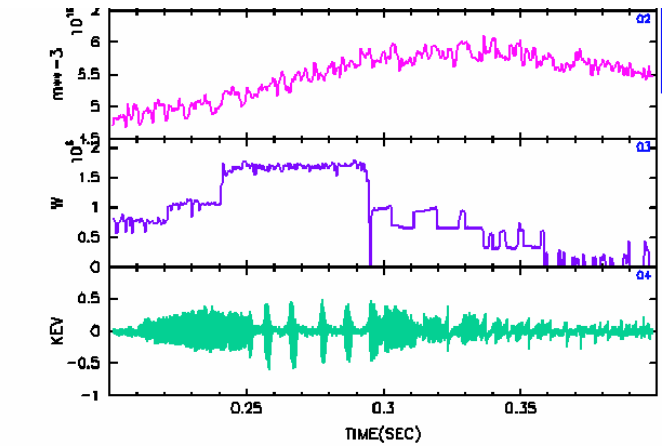

FIG. 4: Electron fishbones in FTU.

This area clearly benefits form better diagnostic capabilities [20], an example of which is given in Fig. 5. Here, reversed shear Alfven eigenmodes (RSAEs) on JT-60U [21] are shown, that lead to a decrease of the neutron rate with respect to the prediction by classical slowing down. This clearly shows that Alfvenic eigenmodes are of potential importance to the fast ion redistribution, especially in advanced scenarios where the poloidal field is weak in the core region. Comparison of Alfvenic MHD activity with theory generally shows that linear stability is relatively well understood, but the nonlinear saturation is difficult to predict quantitatively since important elements, such as the damping rates due to various mechanisms, is not understood equally well.

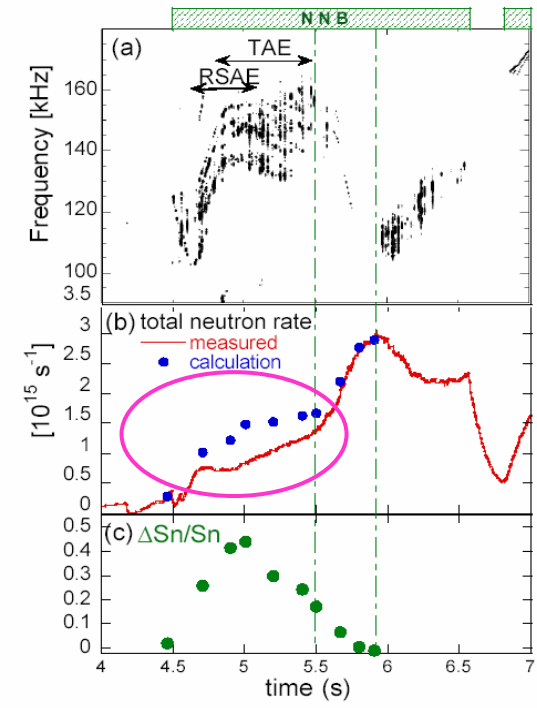

FIG 5: RSAEs on JT-60. A decrease of the neutron rate due to the redistribution of beam ions is clearly seen in traces (b) and (c) during RSAE activity.

Another region in which the interaction of fast ions and MHD modes is of potential importance is the case of the so-called hybrid scenarios, which has flat, elevated central q-profiles. Analysis of the current profile evolution in these scenarios clearly shows that the q-profiles are not consistent with a combination of neoclassical resistivity and bootstrap and NBI-driven current [22]. Often, central MHD modes occur in this type of discharges and thus, several explanations for an interaction between MHD modes and the current profile have been put forward. These include the redistribution of fast beam ions that are supposed to drive current and an excitation of Alfven modes by sidebands of neoclassical tearing modes that would lead to a decreased central current as well [23]. Further evidence for a reduction of fast ion driven current came from an analysis of the current profile in NSTX where clearly, large tearing modes led to a broadening and decrease of efficiency of the NBI-driven current [24]. These mechanisms could finally lead to a non-linear self-organisation of the central current profile in this operating scenario, since on the one hand, MHD mode stability depends on the current profile shape and on the other hand, MHD modes seem to react back on the current profile via the mechanisms discussed above. Several states of the current profile seem to be possible, depending on the type of MHD that provides stationarity (e.g. fishbones, NTMs of different mode number) with distinct difference in performance. For example, sawtooth free hybrid discharges can be obtained in ASDEX Upgrade either with fishbone or (3,2) NTM activity, the latter having a smaller improvement in confinement w.r.t. standard sawtoothing H-mode [25].

3.2. Conventional Heating and Current Drive Scenarios

In this area, a large part of the work was devoted to the experimental proof of NBCD, especially in scenarios where off-axis NBCD is attempted. On ASDEX Upgrade, it was shown that the measured off-axis NBCD profile in high power discharges was not consistent with simulations based on classical slowing down. Instead, an anomalous radial diffusion on the order of 0.5 m^2/s has to be involved to explain the experimental observation, i.e. a broader

current profile that appears to be shifted inward w.r.t. the predictions, as shown in the left part of Fig. 6 [26]. This has led to the hypothesis that the electrostatic turbulence responsible for anomalous transport can also affect fast ions. First theoretical analysis shows that for relevant Kubo numbers, this could indeed be possible.

.

Analysis of far off-axis CD in JT-60U [27], presented in the right part of Fig. 6, clearly showed that current can be driven as far off-axis as ρ=0.8, but again the profile of the driven current was not consistent with the theoretical prediction that in this case showed more inward shifted profiles. This clearly needs resolution in future, especially in view of the prominent role that off-axis NBCD plays in scenario modelling for future experiments such as JT-60SA and ITER.

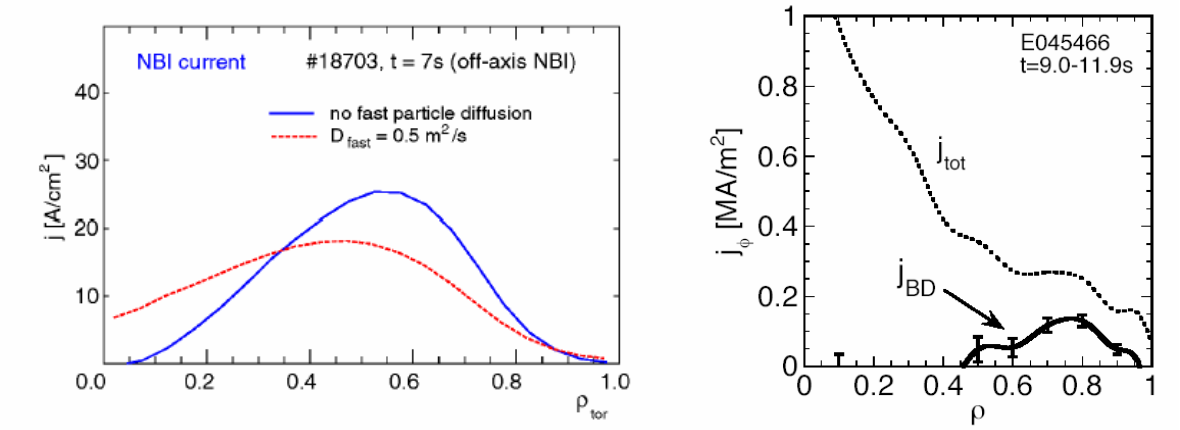

FIG. 6: Off-axis NBCD on ASDEX Upgrade (left, predictions with and without anomalous diffusion, where the case with anomalous diffusion matches the experiment) and on JT-60U. In both cases, discrepancies between measurement and prediction exist

In the area of LHCD, results were presented from JET [28] which show that with local gas puff in front of the antenna, it is possible to create a plasma there sufficient for good coupling.

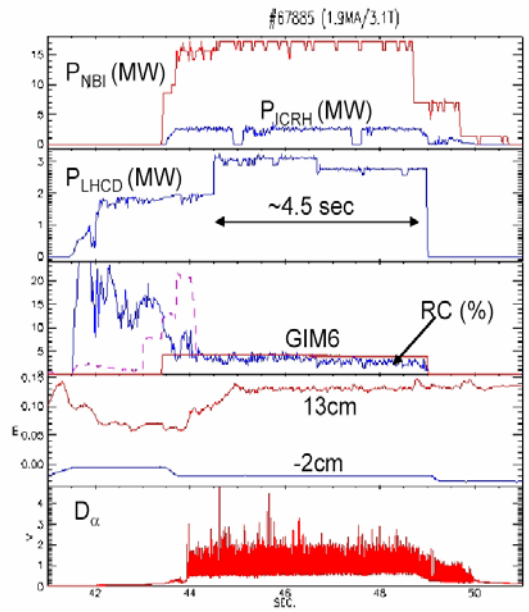

Previous experiments had used CD_4, now also a D_2 puff was shown to be very effective without strong fuelling. Fig. 7 shows an example in which 3 MW of LHCD power were coupled into a strongly heated (~20 MW) ELMy H-mode scenario for 4.5 s. By moving both plasma and grill position, the distance between the separatrix and the grill could be increased to 15 cm, which minimises direct interaction between plasma and grill. This result sheds new light on the use of LHCD in future devices, especially given the lack of efficient off-axis CD schemes for ITER.

FIG.7: Coupling of LHCD power to a JET ELMy H-mode with a distance between grill and separatrix of 15 cm.

3.3 New schemes for new configurations

In this area, schemes are explored to heat plasmas and drive current noninductively in non-tokamak experiments. This is especially pronounced for spherical tori, where the magnetic field is too low for conventional ECRH scenarii and non-inductive start-up is important due to the limited volt seconds available from the central solenoid, which is restricted due to the space limitation in the cenre of the machine. Progress on EBW heating of spherical tori was reported from MAST, where EBW was coupled and clearly increased the stored energy [29]. This scheme was also demonstrated in a conventional tokamak discharge by applying the OXB scheme, previously used on the W7-AS stellarator, on TCV [30].

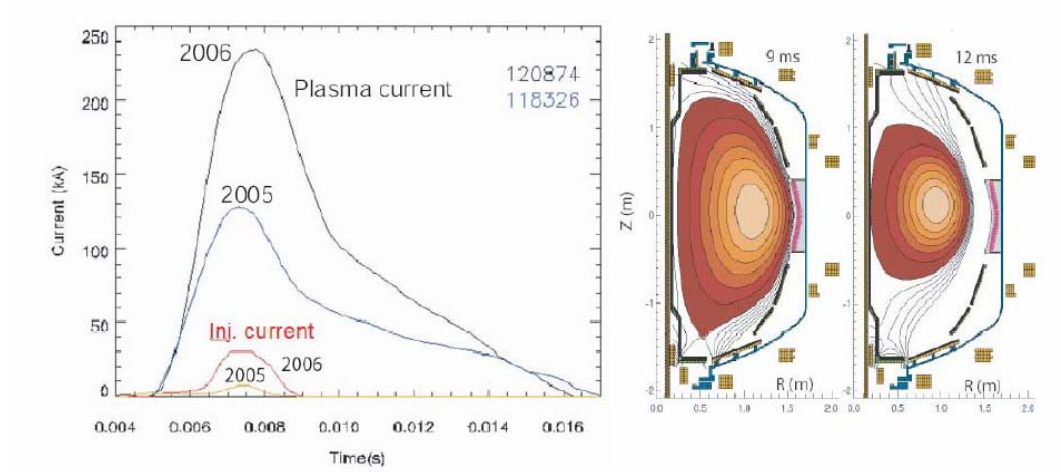

FIG. 8: Transformerless startup in the NSTX spherical torus by coaxial helicity injection, demonstrating the formation of closed flux surfaces by this method.

Transformerless startup experiments were reported from NSTX [31] (by coaxial helicity injection, see Fig. 8) and LATE with ECRH [32]. In both experiments, closed flux surfaces were demonstrated, but an experimental demonstration that this plasma can be ramped up to full parameters is still missing. In both experiments, flux was supplied by the vertical field coils that change their currents to provide equilibrium.

4. Session S: Stability

In the stability session, the main results presented were concerned with the understanding and control of the major MHD instabilities limiting β in present day tokamak experiments, i.e. NTMs for scenarios with monotonic q-profiles and RWMs in scenarios with reversed or strongly elevated shear. In addition, the mitigation of disruptions and ELMs was discussed. ELM physics studies have a strong link to bursty transport, which has been discussed above (section 2.1 of this summary).

4.1 Resistive Wall Modes (RWMs)

In the area of RWMs, new results were presented on rotational suppression of this instability. Previous studies had indicated a relatively high rotation requirement (several percent of the Alfven velocity) at the rational surface of interest to prevent RWMs when the no-wall β-limit is exceeded in DIII-D [33] and JT-60U [34]. Both experiments have now a reduced intrinsic error field (which can seed RWMs due to resonant field amplification), achieved by ferritic inserts in JT-60 U and by active cancellation in DIII-D. Under these circumstances, controlling rotation by a mix of co- and ctr-injected beams (instead of breaking by a helical field in DIII-D, which previously may have served as seed for RWMs itself), the rotational

threshold for RWM onset was found to be greatly reduced (both experiments now report only 0.3 % of the Alfven velocity as necessary condition for RWM suppression). An example is shown in Fig. 9. This has important implications for ITER, where the predicted rotation is only of this order of magnitude. However, better theoretical understanding is needed before a firm extrapolation can be made. Significant progress in active stabilisation of RWMs in low-rotation plasmas was reported form the reversed field pinch experiments RFX [35] and EXTRAP-2TR [36], where sophisticated feedback schemes applying external helical fields successfully widened the operational range of these experiments.

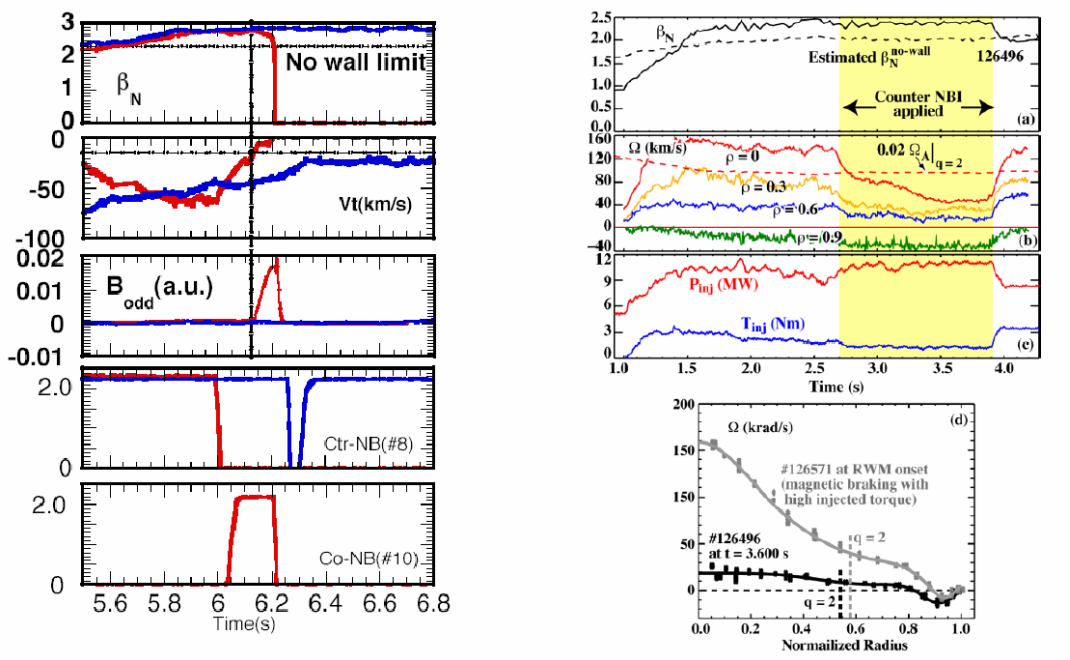

FIG. 9: Experiments on JT-60U (left) and DIII-D (right) showing that rotational stabilisation of RWMs above the no-wall limit is possible at rather low rotation.

4.2 Neoclassical Tearing Modes (NTMs)

The contributions on NTMs focused on the suppression of this instability by local current drive at the resonant surface of interest by ECCD. This method, now envisaged to be used in ITER, is predicted to need phased injection of ECCD into the O-point of the magnetic island in ITER, where the deposition width of the ECCD will be larger than the marginal island size down to which the mode has to be suppressed. This situation is usually not encountered in present day experiments, because of the ρ* scaling of the marginal island width. However, recent experiments in ASDEX Upgrade with broadened ECCD deposition that mimic the ITER situation clearly show the advantage of modulation in this situation [37]. This is shown on the left side of Fig. 10.

Progress was also reported in the area of feedback controlled ECCD deposition during NTM suppression. On DIII-D, the plasma position was varied during (2,1) NTM suppression to track the shift of the resonant surface during β increase by the Shafranov shift (right part of Fig. 10) [38].

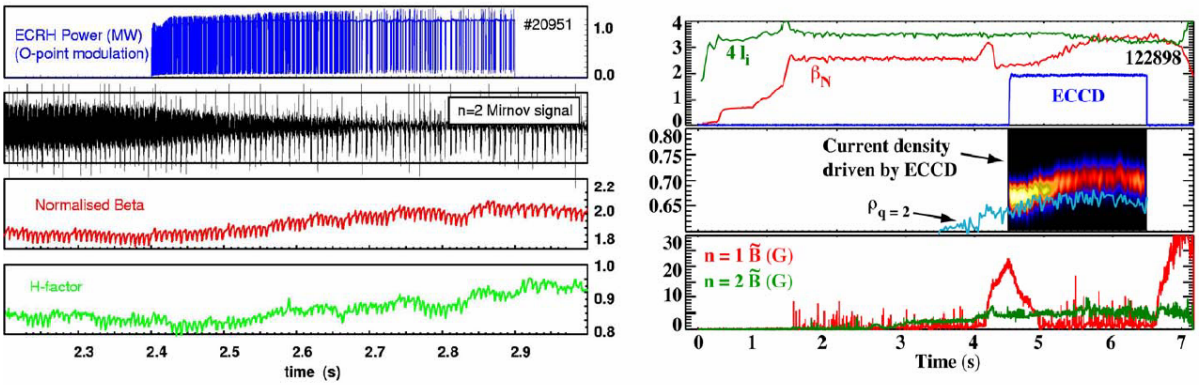

FIG. 10: NTM suppression by ECCD: complete suppression of a (3,2) NTM by phased ECCD in ASDEX Upgrade with broad deposition (left) and feedback controlled deposition during (2,1) NTM suppression in DIII-D.

An important issue that remains to be solved is the extrapolation of the requirements for complete suppression to ITER. This is now commonly described in terms ratio between ECCD current density and bootstrap current density. Experiments on JT-60U showed suppression of a (2,1) NTM at low values of this parameter (down to $j_{ECCD}/j_{bs} = 0.5$) [39], but still the extrapolation to ITER has large uncertainty, ranging between 0.9 [40] and 1.9 [41], depending on the assumptions made about the misalignment of the ECCD in present day experiments. Further coordinated experiments will have to be performed to narrow down these discrepancies.

4.3 Disruptions

In the area of disruptions, the main emphasis was on mitigation of the adverse effects of disruptions, in particular the heat load (not a problem in present day devices, but significant in ITER) and the forces due to halo currents. Both effects have been shown to be mitigated by the introduction of radiating impurities in the disruption phase. The main issue is to supply on a fast time scale a sufficient amount of radiating impurities. Different routes are followed, such as pellets on ASDEX Upgrade [42] or high pressure gas puffs in ASDEX Upgrade, Alcator C-Mod and DIII-D [43]. A study carried out on Alcator C-Mod clearly showed that the mitigation by high pressure noble gas injection becomes more efficient with higher Z.

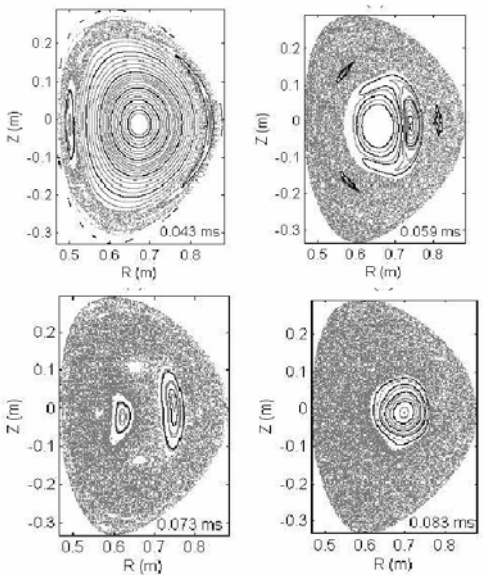

FIG 11: Modeling of the destruction of flux surfaces by MHD modes introduced by rapid edge cooling due to impurity injection in Alcator C-Mod using the NIMROD code.

A related problem is the explanation of the mechanism that leads to the fast disruption. It can be shown that the gas jet does not penetrate to the centre, so that one would not expect central radiation to contribute to the rapid cooling observed. A recent study carried out using the NIMROD code modelling Alcator C-Mod data indicates that the process may be linked to the formation of large scale MHD modes due

to the steepening of the current profile by the edge cooling. Fig. 11 shows results form such a simulation, clearly indicating that in the fully developed phase, the flux surfaces are severely stochastised and the energy and current quench are inevitable in such a situation.

4.4 Edge Localised Modes (ELMs)

In this area, focus is on the one hand on detailed characterisation of the ELM process, on the other hand on the development of scenarios to mitigate the pulsed ELM heat load. ELM physics studies are intimately linked to the characterisation of the filamentary structures as described above in section 2.1. While nonlinear models to describe the ELM process in detail are just starting to be developed, linear stability that predicts the mode onset is now well-established in terms of the peeling-ballooning model that can explain many features of ELM stability [44].

The area of ELM mitigation is largely driven by the worry that standard type I ELMs may lead to unacceptable heat pulses to the ITER divertor. Thus, methods are sought to induce higher frequency, lower energy ELMs without affecting adversely the confinement. These studies necessarily have to cover a large range of operating parameters because the ITER edge will have a unique combination of high density (in terms of the empirical Greenwald limit) and low collisionality. In the area of high density scenarios, JET reported that by carefully adjusting the plasma shape, it was now possible to obtain pure type II ELM phase in this device [45], thus opening the route to a demonstration of scalability of this scenario from ASDEX Upgrade, where it had previously been established.

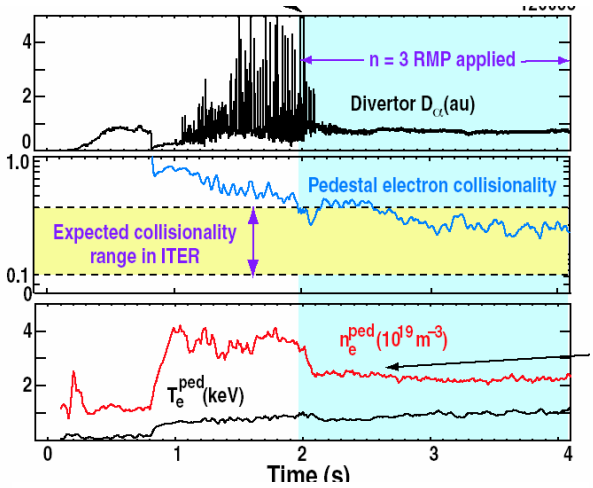

FIG. 12: Suppression of type I ELMs at low collisionality in DIII-D by application of a resonant magnetic perturbation (RMP).

At low collisionality, a new method to suppress ELMs by the application of resonant magnetic perturbations (RMPs) was demonstrated on DIII-D [46]. Previous experiments in this area on JFT-2M and COMPASS-D had been in the type III ELM regime, but DIII-D now clearly shows the possibility to do this in type I ELMy H-mode as well. An example is shown in Fig. 12. It is observed that the application of the RMP leads to a gradual relaxation of the edge pressure gradient, which is thought to be responsible for ELM suppression. However, the impact on global confinement is very small, such that such an interesting, if applicable, could very interesting for ITER. More work is planned, including the installation of RMP coils in other devices and theoretical work to better understand the suppression mechanism.

5. Conclusions

In summary, important progress was reported in all three areas, with a clear orientation towards ITER. However, input from non-tokamak devices continues to play an important role in our general understanding of fusion oriented plasma physics. A general remark is that both in the area of fast particle driven instabilities as well as in the field of ELM physics, linear

stability calculation seem to be well at hand, but the nonlinear part is just being developed. This is urgently needed to make quantitative predictions not only on the onset of instabilities, but also on the nonlinear evolution and thus the impact on confinement. An important new aspect linked to this area is the interaction between MHD modes and the current profile, which also may have the interaction with fast particles as one channel of communication. We expect exciting progress to be reported in Geneva in 2008 in all these areas.

6. References

The papers listed below have been presented at the Conference and can be found at http://www-naweb.iaea.org/napc/physics/FEC/FEC2006/html/index.htm

[1] Grulke, O., et al., Radial Propagation of Eruptive Turbulent Transport Events in the Scrape-Off Layer of Alcator C-Mod, EX/P4-7.

[2] Neuhauser, J. et al., Structure and Dynamics of Spontaneous and Induced ELMs on ASDEX Upgrade, EX/P8-2.

[3] Boedo, J., et al., Particle and Energy Transport in the SOL of DIII-D and NSTX, EX/P4-2.

[4] Pitts, R. et al., On the origin of anomalous radial transport in the tokamak SOL, EX/3-1.

[5] Asakura, N., et al., ELM Propagation and Fluctuations Characteristics in H- and L-mode SOL Plasmas on JT-60U, EX/9-2.

[6] Ohno, N. et al., Bursty Fluctuation Characteristics in SOL/Divertor Plasmas of Large Helical Device, EX/P4-20.

[7] Kirk, A. et al., Evolution of the pedestal on MAST and the implications for ELM power loadings, EX/9-1.

[8] Gunn, J., et al., Links Between Wide Scrape-Off Layers, Large Parallel Flows, and Bursty Transport in Tokamaks, EX/P4-9.

[9] Loarer, T., et al., Gas Balance and Fuel Retention in Fusion Devices, EX/3-6.

[10] Kirschner, A., et al., Material erosion and redeposition during the JET MkIIGB-SRP divertor campaign, EX/3-5.

[11] Allen, S. et al., Transport and Deposition of 13C From Methane Injection Into L- and H-Mode Plasmas in DIII-D, EX/P4-1.

[12] Whyte, D. et al., Hydrogenic fuel recovery and retention with metallic plasma-facing walls in the Alcator C-Mod tokamak, EX/P4-29.

[13] Campbell, D., et al., Critical Physics Issues for Tokamak Power Plants, FT/1-1.

[14] Marmar, E., et al., Operation of Alcator C-Mod with High-Z Plasma Facing Components with and without Boronization, EX/3-4.

[15] Dux, R. et al., Tungsten as first wall material in ASDEX Upgrade, EX/3-3Ra.

[16] Mazzitelli, G., et al., Lithium as a Liquid Limiter in FTU, EX/P4-16.

[17] Mirnov, S.., et al., Lithium experiment in tokamak T-11M and concept of limiter tokamak-reactor, EX/P4-17.

[18] Ohyabu, N., et al., Super Dense Core Plasma due to Internal Diffusion Barrier in LHD, EX/8-1.

[19] Zonca, F., et al., Electron fishbones: theory and experimental evidence, TH/3-2.

[20] Heidbrink, W., et al., Alfven Instabilities in DIII-D: Fluctuation Profiles, Thermal-Ion Excitation, and Fast-Ion Transport, EX/6-3

[21] Ishikawa, M., et al., Confinement Degradation of Energetic Ions due to Alfvén Eigenmodes in JT-60U Negative-Ion-Based Neutral Beam Injection Plasmas, EX/6-2.

[22] Casper, T., et al., Evidence for Anomalous Effects on the Current Evolution in Tokamak Operating Scenarios, EX/P6-4.

[23] Chu, M., et al., Maintaining the Quasi-Steady State Central Current Density Profile in Hybrid Discharges, EX/1-5.

[24] Medley, S., et al., Investigation of Collective Fast Ion Instability-induced Redistribution or Loss in NSTX, EX/P6-13.

[25] Stober, J., et al., Physics studies of the improved H-mode scenario in ASDEX Upgrade, EX/P1-7.

[26] Günter, S., et al., Fast Particle Physics on ASDEX Upgrade, EX/6-1.

[27] Suzuki, T., et al., Off-axis Current Drive and Current Profile Control in JT-60U, EX/6-4.

[28] Ongena, J., et al., Recent progress in JET on Heating and Current Drive studies in view of ITER, EX/P6-9.

[29] Shevchenko, V., et al., Electron Bernstein Wave Heating Experiments on MAST, EX/P6-22.

[30] Pochelon, A., et al., Electron Bernstein Wave Heating of High Density H-modes in the TCV Tokamak, EX/P6-2.

[31] Raman, R. et al., Solenoid-free Plasma Start-up in NSTX using Transient CHI, EX/P8-16.

[32] Tanaka, H., et al., Spherical Tokamak Startup and Formation by ECH without Central Solenoid on LATE, EX/P6-6.

[33] Garofalo, A., et al., Active Control of Resistive Wall Modes in High Beta, Low Rotation DIII-D Plasmas, EX/7-1Ra.

[34] Takechi, M. et al., Plasma Rotation and Wall effects on Resistive Wall Mode in JT-60U, EX/7-1Rb.

[35] Martini, P., et al., Overview of RFX-mod results with active MHD control, EX/7-3.

[36] Drake, J., et al., Experiments on feedback control of multiple resistive wall modes comparing different active coil arrays and sensor types, EX/P8-11.

[37] Zohm, H., et al., Control of MHD Instabilities by ECCD: ASDEX Upgrade Results and Implications for ITER, EX/4-1Rb.

[38] Prater, R., et al., Prevention of the 2/1 Neoclassical Tearing Mode in DIII-D, EX/4-2.

[39] Isayama, A., et al., Active Control of Neoclassical Tearing Modes toward Stationary High-Beta Plasmas in JT-60U, EX/4-1Ra.

[40] La Haye, R., et. al., Evaluating Electron Cyclotron Current Drive Stabilization of Neoclassical Tearing Modes in ITER: Implications of Experiments in ASDEX-U, DIII-D, JET, and JT-60U, EX/P8-12.

[41] Sauter, O., et al., Partial Stabilization and Control of Neoclassical Tearing Modes in Burning Plasmas, TH/P3-10.

[42] Pautasso, G., et al., Mitigated Plasma Shut-Down with Fast Impurity Puff on ASDEX Upgrade, EX/P8-7.

[43] Granetz, R., et al., Gas Jet Disruption Mitigation Studies on Alcator C-Mod and DIII-D, EX/4-3.

[44] Snyder, P., et al., Stability and Dynamics of the Edge Pedestal in the Low Collisionality Regime: Physics Mechanisms for Steady-State ELM-Free Operation, TH/4-1Ra.

[45] Watkins, M., et al., Overview of JET Results, OV/1-3.

[46] Moyer, R., et al., Edge Localized Mode Control in DIII-D Using Magnetic Perturbation-Induced Pedestal Transport Changes, EX/9-3.